

Supporting Information

Inverse and highly selective separation of CO₂/C₂H₂ on a thulium-organic framework

Deyun Ma,^{ab} Zhi Li,^c Jiaying Zhu,^d Yiping Zhou,^a Lilin Chen,^a Xufeng Mai,^a Meilin

Liufu,^a Yinbing Wu,^a Yingwei Li^{b}*

*^a School of Food and Pharmaceutical Engineering, Zhaoqing University, Zhaoqing
526061, China.*

*^b State Key Laboratory of Pulp and Paper Engineering, School of Chemistry and
Chemical Engineering, South China University of Technology, Guangzhou 510640,
China. E-mail: liyw@scut.edu.cn*

*^c Shandong Provincial Key Laboratory of Molecular engineering, QiLu University of
Technology (Shandong Academy of Sciences), Jinan 250353, China.*

^d Department of Chemistry, Fudan University, Shanghai 200433, China.

Experimental

2,5-dihydroxyterephthalic acid and $\text{Tm}(\text{NO}_3)_3 \cdot 6(\text{H}_2\text{O})$ were purchased from Aladdin company. 2,2'-Dimethyl-4,4'-bipyridine was synthesized following the reported procedures.¹

Synthesis of $\{[\text{Tm}_2(\text{OH}-\text{bdc})_2(\mu_3-\text{OH})_2(\text{H}_2\text{O})_2] \cdot 11\text{H}_2\text{O}\}_n$: To an aqueous solution (12 mL and pH = 7-8) of 2,5-dihydroxyterephthalic acid (0.060 g, 0.3 mmol), $\text{Tm}(\text{NO}_3)_3 \cdot 6(\text{H}_2\text{O})$ (0.139 g, 0.3 mmol) and 2,2'-dimethyl-4,4'-bipyridine (0.028 g, 0.15 mmol) were added. The mixed solution was sealed in a Teflon reactor (23 mL) and kept at 100 °C for 24 h. Finally, yellow crystals were collected (yield: 78%). Anal. Calcd for $\text{C}_{16}\text{H}_{36}\text{Tm}_2\text{O}_{27}$ (**1**): C, 19.2; H, 3.6. Found: C, 19.6; H, 3.3. IR (KBr pellet) (cm^{-1}): 3462(vs), 2941(m), 2902(w), 1632(vs), 1510(m), 1475(vs), 1392(w), 1246(s), 1116(m), 1058(w), 875(w), 788(s), 602(w), 560(w), 452(w), 416(m) (Fig. S1).

X-ray crystal structural determination: The crystal data of **1** were collected on a Bruker Apex II CCD diffractometer at 50 kV and 30 mA with $\text{MoK}\alpha$ radiation ($\lambda = 0.71073 \text{ \AA}$). The crystal was kept at 150 K during the measurement. Data collection and reduction were performed using the APEX II software.^{2a} The crystal structure of **1** was solved using direct methods followed by least-squares on F^2 using SHELXTL.^{2b} Non-hydrogen atoms were refined with independent anisotropic displacement parameters and hydrogen atoms attached to carbon and oxygen were placed in geometrically idealized positions and refined using the riding model. The routine SQUEEZE (PLATON) was applied to the structure in order to remove diffuse electron density associated with badly disordered water molecules.^{2c} O8, O16, O17 and O18 were disordered and they were split into two sets of positions, with occupancy ratios of 0.491(10):0.509(10), 0.613(8):0.387(8), 0.5:0.5, and 0.504(5):0.496(5), respectively. The TOPOS software was used to topologically analyze **1**.^{2d,2e} The more detail information is listed in the CIF file. Crystal data, as well as detail of data collection and refinement are shown in Table S1. Selected bond lengths and bond angles of **1** are summarized in Table S2.

Material characterization: Elemental analyses were performed on a Vario EL III Elemental Analyzer. IR spectra were obtained on a Shimadzu IR-440 spectrometer in the range of 4000-400 cm^{-1} (KBr disk). Thermogravimetric analysis (TGA) was carried out on an automatic simultaneous thermal analyzer (DTG-60, Shimadzu) under N_2 atmosphere from 25 to 800 $^{\circ}\text{C}$ with a heating rate of 10 $^{\circ}\text{C}/\text{min}$. Powder X-ray diffraction patterns (PXRD) were measured by using a Bruker AXS D8-Advance diffractometer with $\text{Cu-K}\alpha$ ($\lambda = 1.5418 \text{ \AA}$) radiation. The simulated pattern was produced using the Mercury V1.4 program and single-crystal diffraction data.

Gas adsorption measurements: CO_2 , C_2H_2 , and N_2 adsorption isotherms at different temperatures were measured on a Quantachrome Autosorb-iQ instrument under pressures ranging from 0 to 100 kPa. Before each run, about 80 mg of samples were outgassed at 90 $^{\circ}\text{C}$ for 18 h or at 180 $^{\circ}\text{C}$ for 12 h under vacuum to obtain **1a** or **1a'**, respectively. Ultrahigh-purity C_2H_2 (99.99%), CO_2 (99.99%), and N_2 (99.99%) were used. Pore size distribution (PSD) data were obtained from the N_2 adsorption isotherm at 77 K based on the nonlocal density functional theory (NLDFT) model.³

Breakthrough experiments: The breakthrough experiments were performed at room temperature on a self-made dynamic breakthrough setup as show in Fig. S2. A stainless-steel column (100 mm in length and 6 mm in diameter) was used for sample packing. Before the breakthrough experiment, 200 mg of sample was packed into the column. The flow rate (2 mL/min) of $\text{CO}_2/\text{C}_2\text{H}_2$ (1:2, v/v) mixture and pressure were controlled by using a pressure-control valve and a mass flow controller. The outlet gas from the column was analyzed using a chromatography with a Porapak Q column (3.15 m in length and 3 mm in diameter) and a thermal conductivity detector (TCD). Helium (23 mL/min) was used as the carrier gas.

Theoretical simulations: The Dmol³ code of Material Studio software was used to calculate the geometry optimization of CO_2 and/or C_2H_2 molecule under vacuum

condition.^{4a} During the simulated annealing, the gas molecule is able to explore the lowest-energy conformation with the continuously decreased temperature.^{4b} Then a DFT geometry optimization procedure was used to gain the performance of gas within the **1a** and **1a'**, respectively. During the simulation, **1** was fixed, and the gas molecule was flexible and could move around. The PBE GGA density functional was used in the above calculations.^{4c,4d}

The adsorption of CO₂ and C₂H₂ in the pores of activated **1** (**1a** and **1a'**) were calculated by using the Grand-canonical Monte Carlo (GCMC) at 1 bar and 298 K.^{4c,4e,4f} CO₂ was regarded as a rigid linear molecule with 1.16 Å of C–O bond length. The LJ potential parameters of the O atom ($\sigma_O = 3.05$ Å and $\varepsilon_O/\kappa_B = 79.0$ K) and C atom ($\sigma_C = 2.80$ Å and $\varepsilon_C/\kappa_B = 27.0$ K) in the CO₂ molecule were taken from the TraPPE force field.^{4d} Partial point charges were $q_O = -0.35e$ and $q_C = 0.70e$. The C₂H₂ molecule was treated as united-atom model with the Lennard-Jones interaction parameters of $\sigma = 3.8$ Å and $\varepsilon = 0.115$ kJ mol⁻¹.^{4g}

Ideal Adsorbed Solution Theory (IAST): In practice, it is difficult to evaluate the gas adsorption selectivity of an adsorbent directly. The co-adsorption or breakthrough measurements are the two main methods. However, the adsorption selectivity of gas mixtures can be predicted effectively by IAST according to the isotherms of single component gases.⁵ IAST was first proposed by Myers and Prausnitz^{5a}, which requires that the adsorption model must be thermodynamic consistent. In this work, IAST was applied to forecast the adsorption selectivity of CO₂/C₂H₂ binary mixtures. The adsorption selectivity is defined as:^{5c}

$$S = \frac{x_1 y_2}{x_2 y_1}$$

where y and x are the molar fraction in gas phase and adsorbed phase, respectively.

The isosteric heat, Q_{st} : The isosteric heats of C₂H₂ and CO₂ adsorption, Q_{st} , defined as:⁶

$$Q_{st} = RT^2 \left(\frac{\partial \ln P}{\partial T} \right)$$

were ascertained by the Clausius-Clapeyron equation. The gas adsorption isotherms obtained at 273, 298 and 318 K were fitted by the double Langmuir (DL) equation, respectively.

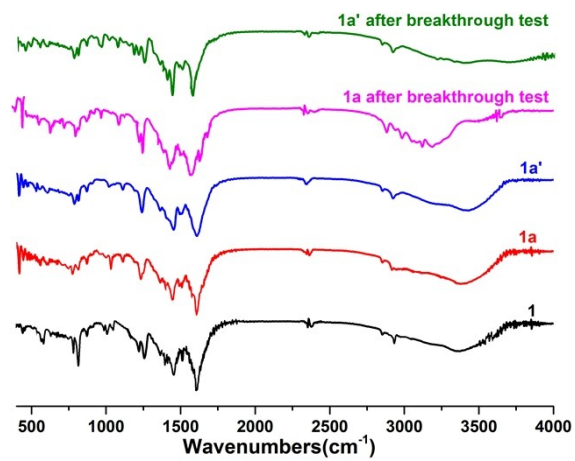


Figure S1. IR spectra of **1**, **1a**, and **1a'** before or after breakthrough test.

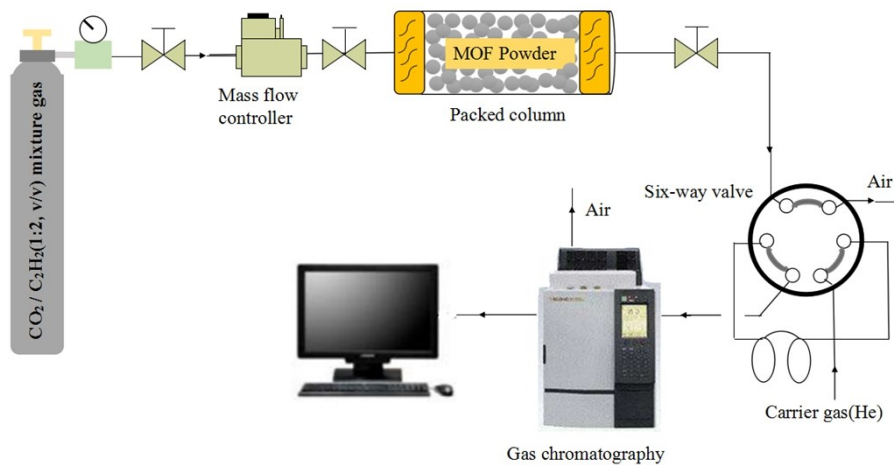


Figure S2. The self-assembly apparatus for breakthrough experiments.

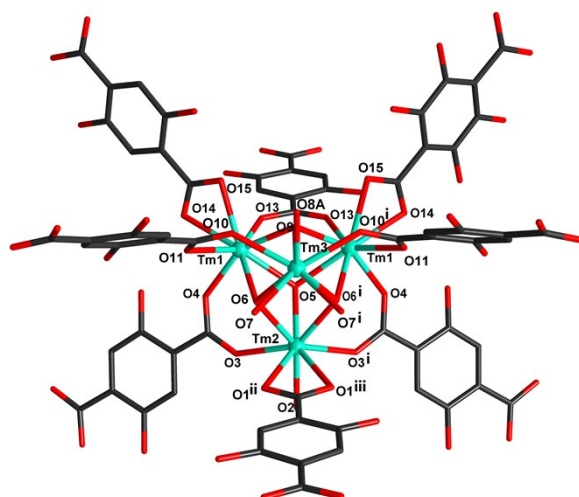


Figure S3. The coordination environment of Tm(III) ions in **1**. All H atoms were omitted for clarity. Color codes: Tm, cyan; O, red; C, black. Symmetry codes: i = x, 1-y, z; ii = 1+x, 0.5-y, z; iii = 1+x, y, z.

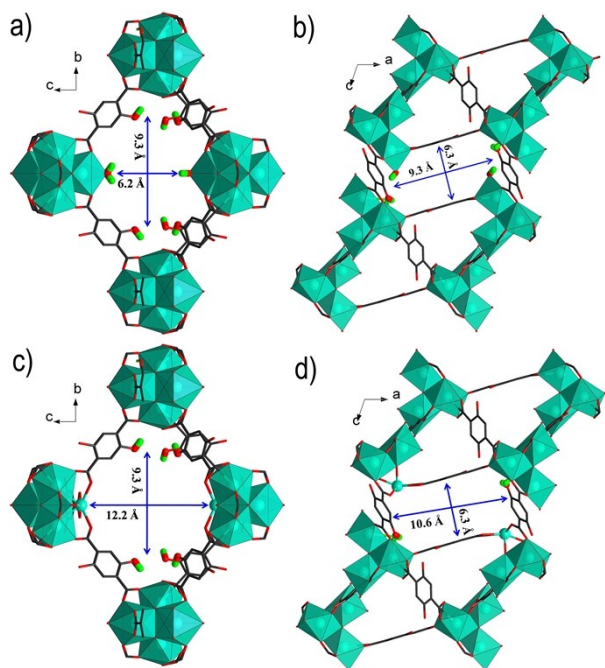


Figure S4. (a, b): View of the pore geometry and aperture sizes of **1a** along the *a* and *b*-axis; (c, d): view of the pore geometry and aperture sizes of **1a'** along the *a* and *b*-axis. Color codes: Tm, cyan; O, red; H, green.

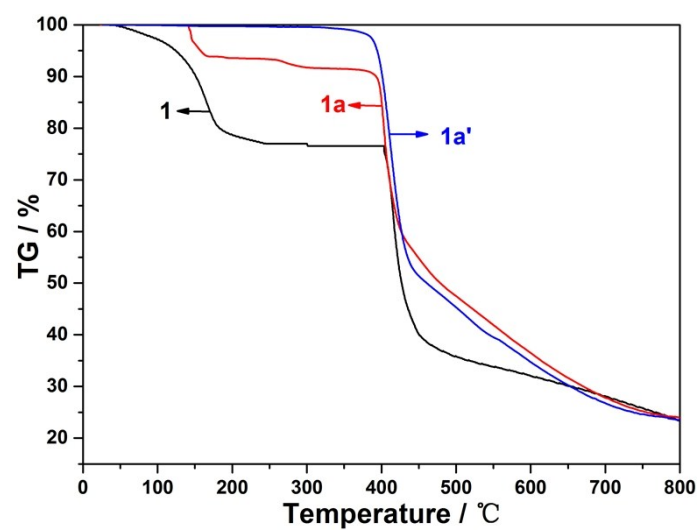


Figure S5. Thermogravimetric curves of **1**, **1a** and **1a'**.

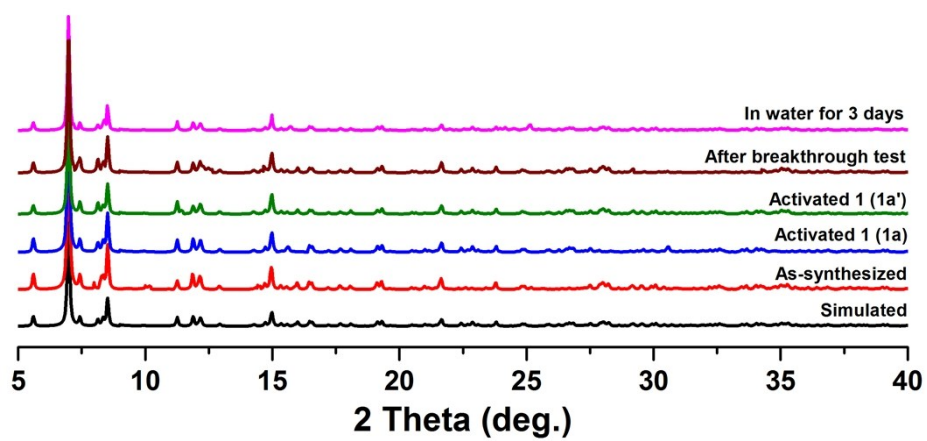


Figure S6. PXRD patterns of **1** samples.

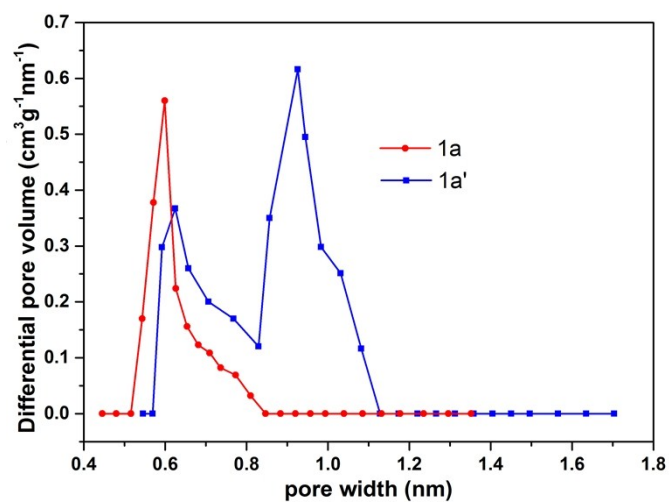


Figure S7. Pore size distribution of **1a** and **1a'** based on the NLDFT model.

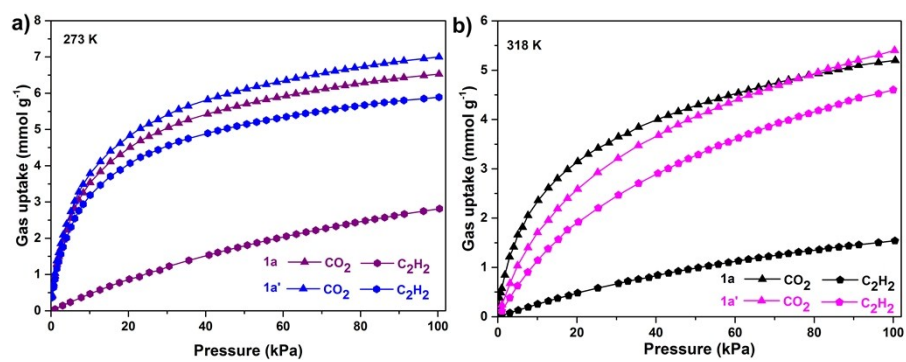


Figure S8. CO₂ and C₂H₂ adsorption isotherms for **1a** and **1a'** at 273 K a) and 318 K b), respectively.

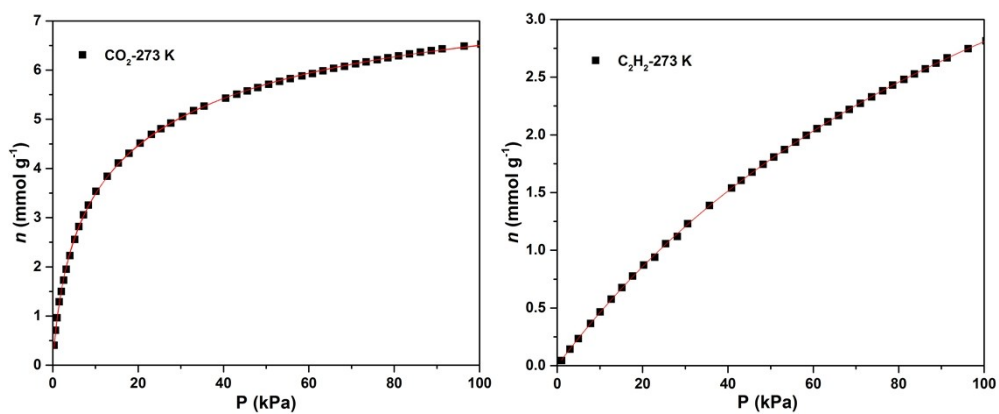


Figure S9. The graphs of the double Langmuir (DL) equation fit for adsorption of CO₂ and C₂H₂ on **1a** at 273 K.

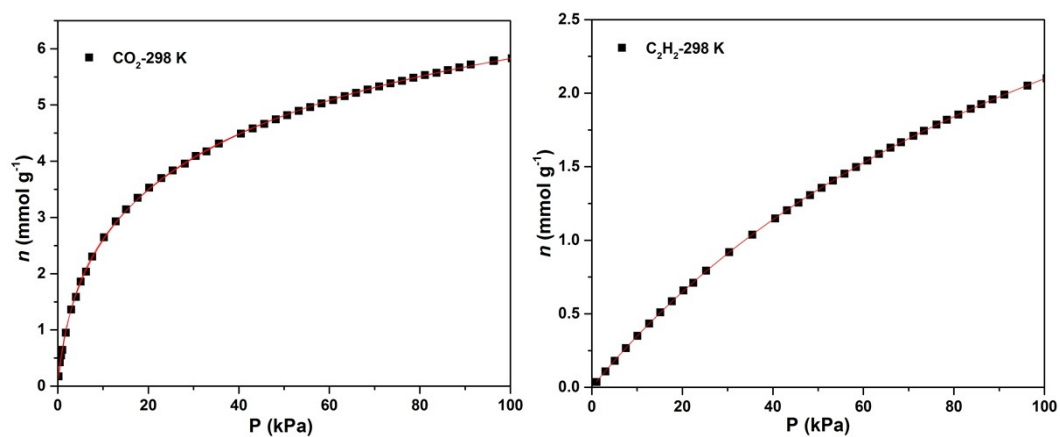


Figure S10. The graphs of the double Langmuir (DL) equation fit for adsorption of CO₂ and C₂H₂ on **1a** at 298 K.

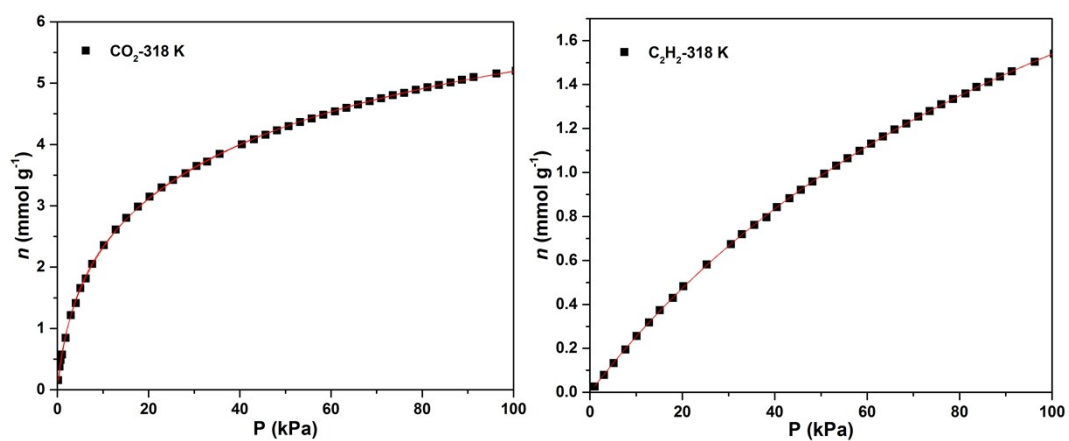


Figure S11. The graphs of the double Langmuir (DL) equation fit for adsorption of CO₂ and C₂H₂ on **1a** at 318 K.

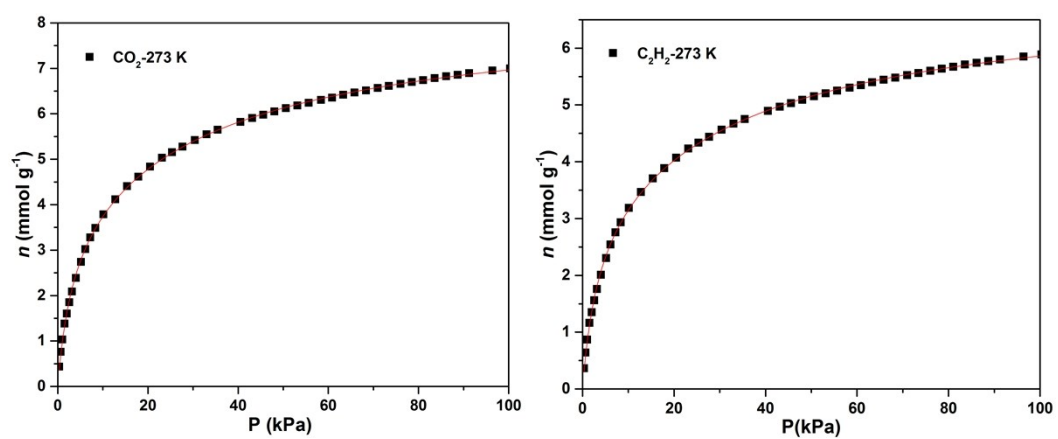


Figure S12. The graphs of the double Langmuir (DL) equation fit for adsorption of CO₂ and C₂H₂ on **1a'** at 273 K.

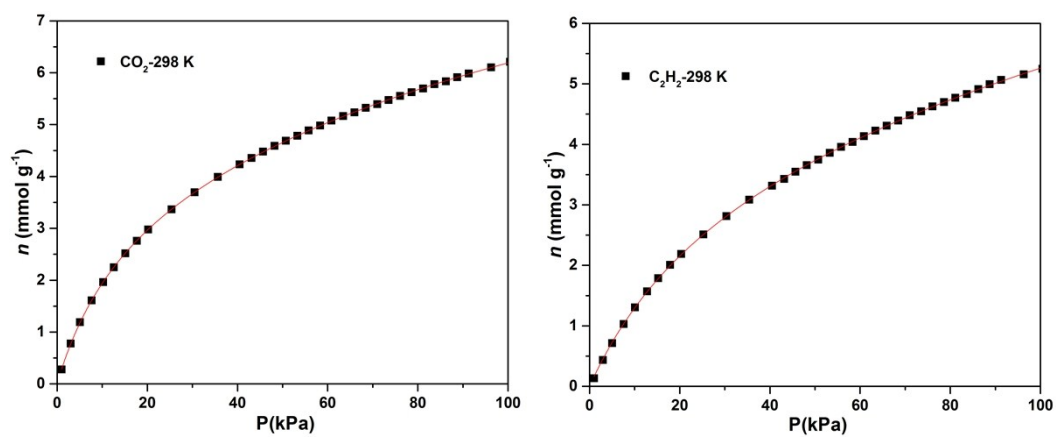


Figure S13. The graphs of the double Langmuir (DL) equation fit for adsorption of CO₂ and C₂H₂ on **1a'** at 298 K.

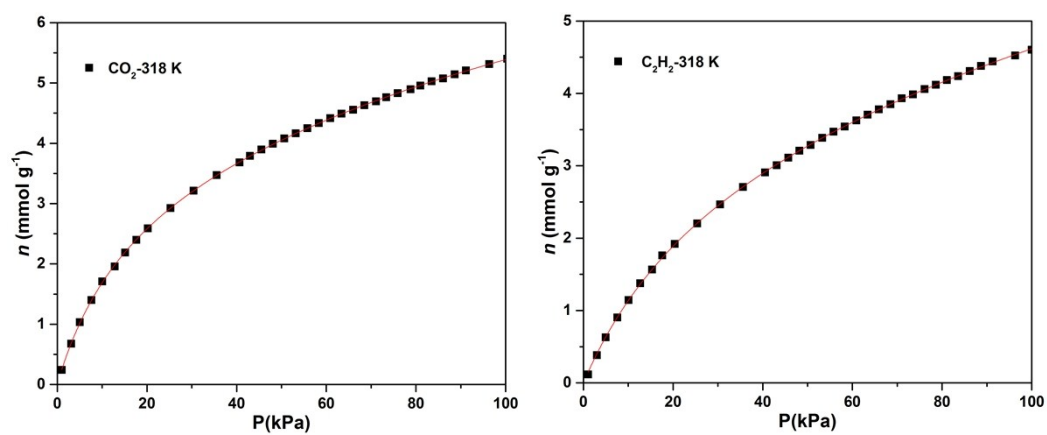


Figure S14. The graphs of the double Langmuir (DL) equation fit for adsorption of CO₂ and C₂H₂ on **1a'** at 318 K.

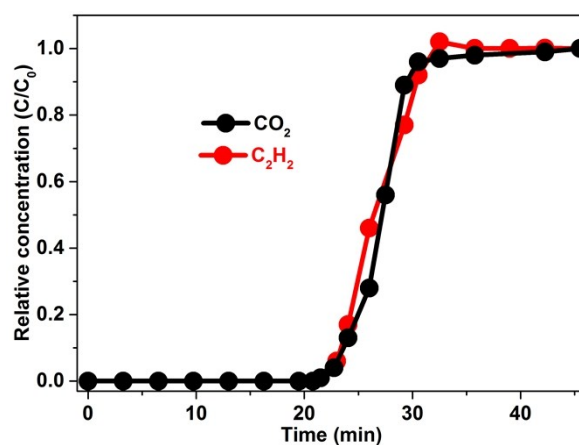


Figure S15. Experimental breakthrough curves of a 1:2 (v/v) gas mixture of CO₂ and C₂H₂ on **1a'** at 298 K and 1.0 bar.

Table S1. Crystallographic data of complex 1.

Empirical formula	C ₁₆ H ₁₄ O ₁₆ Tm ₂	Z	4
Formula weight	800.13	D (Mg.m ³)	1.191
Temperature (K)	150	μ (mm ⁻¹)	3.991
Size (mm)	0.22×0.20×0.18	Reflections collected/unique	29181/8202
Crystal system	monoclinic	<i>R</i> _{int}	0.0572
Space group	<i>P2</i> ₁ / <i>m</i>	<i>F</i> (000)	1504
a (Å)	13.3432(6)	θ (°)	1.290-25.187
b (Å)	21.1879(9)	Goodness-of-fit on <i>F</i> ²	0.934
c (Å)	16.6505(9)	<i>R</i> (<i>I</i> >2σ)	<i>R</i> ₁ = 0.0278
α (°)	90		w <i>R</i> ₂ = 0.0599
β (°)	108.6130(10)		
γ (°)	90	<i>R</i> (all data)	<i>R</i> ₁ = 0.0354
			w <i>R</i> ₂ = 0.0620
V (Å ³)	4461.1(4)	Largest diff. peak and hole (Å ⁻³)	1.56, -2.27

$$R = \sum(|F_o| - |F_c|) / \sum |F_o|$$

$$wR = [\sum w(F_o^2 - F_c^2)^2 / \sum w(F_o^2)]^{1/2}$$

Table S2. Selected bond lengths (Å) and bond angles (°) for **1**.

1			
Tm(1)-O(4)	2.242(3)	Tm(1)-O(5)	2.359(3)
Tm(1)-O(6) ⁱ	2.348(3)	Tm(1)-O(9)	2.289(3)
Tm(2)-O(1) ⁱⁱ	2.410(3)	Tm(2)-O(1) ⁱⁱⁱ	2.410(3)
Tm(2)-O(2) ⁱⁱ	2.348(5)	Tm(2)-O(3) ⁱ	2.322(3)
Tm(3)-O(6) ⁱ	2.322(3)	Tm(3)-O(7) ⁱ	2.333(3)
Tm(3)-O(10) ⁱ	2.343(3)	Tm(3)-O(9) ⁱ	2.365(4)
O(4)-Tm(1)-O(5)	84.00(12)	O(4)-Tm(1)-O(6) ⁱ	84.19(11)
O(4)-Tm(1)-O(9)	152.65(12)	O(4)-Tm(1)-O(11)	84.82(14)
O(4)-Tm(1)-O(13)	96.99(13)	O(4)-Tm(1)-O(14)	74.61(11)
O(1) ⁱⁱⁱ -Tm(2)-O(1) ⁱⁱ	53.87(14)	O(2) ⁱⁱⁱ -Tm(2)-O(1) ⁱⁱ	79.40(16)
O(1) ⁱⁱⁱ -Tm(2)-O(1) ⁱⁱ	112.8(4)	O(3) ⁱ -Tm(2)-O(1) ⁱⁱⁱ	112.8(4)
O(6) ⁱ -Tm(3)-O(6)	68.91(14)	O(6)-Tm(3)-O(7) ⁱ	116.83(14)
O(7) ⁱ -Tm(3)-O(7)	70.6(2)	O(10) ⁱ -Tm(3)-O(9)	75.05(10)

Symmetry codes: i = x, 1-y, z; ii = 1+x, 0.5-y, z; iii = 1+x, y, z.

Table S3. The uptakes of CO₂, C₂H₂ and adsorption selectivities of CO₂/C₂H₂ (1:2 CO₂:C₂H₂, v/v) over various adsorbents for inverse adsorption of CO₂ over C₂H₂.

Adsorbents	<i>T</i> (K)	<i>P</i> (kPa)	CO ₂ uptake (mmol g ⁻¹) ^a	C ₂ H ₂ uptake (mmol g ⁻¹) ^a	Selectivity (IAST) ^b	<i>q</i> (CO ₂ / C ₂ H ₂) ^c	<i>Ref.</i>
CD-MOF-1	298	100	0.55/2.87	0.15/2.23	6.6	3.7	7
CD-MOF-2	298	100	1.10/2.65	0.03/2.03	16.0	36.7	7
SIFSIX-3-Ni	298	100	1.07/2.70	0.09/3.30	7.7	11.9	8
[Mn(bdc)(dpe)]	273	91	0.012/2.09	0.002/0.33	9.0	6.0	9
Ionic crystal	278	100	0.005/0.51	0.002/0.02	4.8 ^d	2.5	10
[Co(HL)]	195	100	10.69	6.41	1:0.58 ^e	-	11
1a	298	100	0.19/5.83	0.01/2.1	17.5	19.0	this work
1a'	298	100	0.05/6.21	0.03/5.25	1.65	1.67	this work

^a Gravimetric uptake (mmol g⁻¹) at 0.2 kPa/100 kPa, except [Mn(bdc)(dpe)] at 0.2 kPa/91 kPa. ^b Selectivity calculated from IAST for the CO₂/C₂H₂ (1:2, v/v) mixture at 100 kPa, except CO₂/C₂H₂ (1:1, v/v) for [Mn(bdc)(dpe)]. ^c Ratio of the adsorption capacity of CO₂/C₂H₂ at 0.2 kPa. ^d Selectivity calculated from CO₂ and C₂H₂ uptake at 1.0 bar. ^e CO₂/C₂H₂ uptake ratio.

Table S4. Fitting parameters of the double Langmuir model of **1a**.

Adsorbates	q_{m1}	k_1	q_{m2}	k_2	R^2
CO ₂ (273 K)	4.42214	0.02741	3.36450	0.30537	0.9997
C ₂ H ₂ (273 K)	0.01715	0.06786	6.55793	0.00742	0.9999
CO ₂ (298 K)	5.38268	0.01588	2.61977	0.25433	0.9997
C ₂ H ₂ (298 K)	4.78435	0.00769	0.02289	0.03666	0.9999
CO ₂ (318 K)	4.79293	0.01622	2.31160	0.25751	0.9997
C ₂ H ₂ (318 K)	3.51283	0.00779	$3.3297 \times e^{-10}$	$1.17749 \times e^{-9}$	0.9999

Table S5. Fitting parameters of the double Langmuir model of **1a'**.

Adsorbates	q_{m1}	k_1	q_{m2}	k_2	R^2
CO ₂ (273 K)	4.74053	0.02741	3.60676	0.30537	0.9997
C ₂ H ₂ (273 K)	3.98876	0.02741	3.03479	0.30537	0.9997
CO ₂ (298 K)	8.68670	0.0050	3.78179	0.06752	0.9999
C ₂ H ₂ (298 K)	3.99299	0.0349	11.04606	0.00243	0.9999
CO ₂ (318 K)	7.73402	0.00464	3.3839	0.06592	0.9999
C ₂ H ₂ (318 K)	3.47495	0.03519	9.96689	0.00237	0.9999

Table S6. Comparison of breakthrough experiments parameters of SIFSIX-3-Ni, CD-MOF-1, CD-MOF-2 and **1a**.

Adsorbents	T (K)	Sample weight (mg)	Total flow (mL min ⁻¹)	CO ₂ /C ₂ H ₂ mixture	Breakthrough time (min)	Selectivity (IAST)	<i>Ref.</i>
SIFSIX-3-Ni	298	500	10.0	1:2, v/v	100	6.6	8
CD-MOF-1	298	590	2.0	1:2, v/v	116	16.0	7
CD-MOF-2	298	590	2.0	1:2, v/v	160	7.7	7
1a	298	200	2.0	1:2, v/v	45	17.5	this work

References

- [1] D. Ma, Y. Li, Z. Li, *Chem. Commun.*, 2011, **47**, 7377-7379.
- [2] (a) Bruker. APEX II Software, version 6.3.1; Bruker AXS Inc: Madison, Wisconsin, USA, 2004; (b) G. M. Sheldrick, A short history of SHELX. *Acta Crystallogr., Sect. A*, 2008, **64**, 112–122; (c) A. L. Spek, PLATON, A Multipurpose Crystallographic Tool; Utrecht University: Utrecht, The Netherlands, 2005; (d) V. A. Blatov, A. P. Shevchenko, D. M. Proserpio, *Cryst. Growth Des.*, 2014, **14**, 3576–3586; (e) G. Nandi, R. Thakuria, H. M. Titi, R. Patra, I. Goldberg, *CrystEngComm*, 2014, **16**, 5244–5256.
- [3] Y. Zhu, S. Murali, M. D. Stoller, K. J. Ganesh, W. Cai, P. J. Ferreira, A. Pirkle, R. M. Wallace, K. A. Cychosz, M. Thommes, D. Su, E. A. Stach, R. S. Ruoff, *Science*, 2011, **332**, 1537-1541.
- [4] (a) DMol3, v. Accelrys, Inc, San Diego, 2005. (b) R. Babarao, J. Jiang, *J. Phys. Chem. C*, 2009, **113**, 18287-18291; (c) J. P. Perdew, Y. Wang, *Phys. Rev. B*, 1992, **45**, 13244-13249; (d) P. Horcajada, C. Serre, G. Maurin, N. A. Ramsahye, F. Balas, M. Vallet-Regi, M. Sebban, F. Taulelle, G. Férey, *J. Am. Chem. Soc.*, 2008, **130**, 6774-6780; (e) Q. Yang, C. J. Zhong, *J. Phys. Chem. C*, 2005, **24**, 11862-11864; (f) D. Wu, C. Wang, B. Liu, Q. Yang, C. Zhong, *AIChE J.*, 2012, **58**, 2078-2084; (g) P. Kr. Ghorai, S. Yashonath, P. Demontis, G. B. Suffritti, *J. Am. Chem. Soc.*, 2003, **125**, 7116-7123.
- [5] A.L. Myers, J.M. Prausnitz, *AIChE J.*, 1965, **11**, 121-127; (b) K. Sumida, D.L. Rogow, J.A. Mason, T.M. McDonald, E.D. Bloch, Z.R. Herm, T.H. Bae, J.R. Long, *Chem. Rev.*, 2012, **112**, 724-781; (c) Y. Chen, D. Lv, J. Wu, J. Xiao, H. Xi, Q. Xia, Z. Li, *Chem. Eng. J.*, 2017, **308**, 1065-1072; (b) Y. Wu, H. Chen, D. Liu, Y. Qian, H. Xi, *Chem. Eng. Sci.*, 2015, **124**, 144-153; (c) J. Chen, L.S. Loo, K. Wang, *J. Chem. Eng. Data*, 2011, **56**, 1209-1212; (d) F.A. Kloutse, A. Hourri, S. Natarajan, P. Benard, R. Chahine, *Sep. Purif. Technol.*, 2018, **197**, 228-236; (e) F.A. Kloutse, A. Hourri, S. Natarajan, P. Benard, R. Chahine, *Micropor. Mesoporo. Mater.*, 2018, **271**, 175-185.

- [6] (a) L. Zhang, K. Jiang, Y. Yang, Y. Cui, B. Chen, G. Qian, *J. Solid State Chem.*, 2017, **255**, 102-107; (b) H. Pan, J.A. Ritter, P.B. Balbuena, *Langmuir*, 1998, **14**, 6323-6327; (c) A. F. Kloutse, R. Zacharia, D. Cossement, R. Chahine, R. Balderas-Xicohtencatl, H. Oh, B. Streppel, M. Schlichtenmayer, M. Hirsche, *Appl. Phys. A*, 2015, **121**, 1417-1424.
- [7] L. Li, J. Wang, Z. Zhang, Q. Yang, Y. Yang, B. Su, Z. Bao, Q. Ren, *ACS Appl. Mater. Interfaces*, 2019, **11**, 2543-2550.
- [8] K. J. Chen, H. S. Scott, D. G. Madden, T. Pham, A. Kumar, A. Bajpai, M. Lusi, K. A. Forrest, B. Space, J. J. Perry IV, M. J. Zaworotko, *Chem*, 2016, **1**, 753-765.
- [9] M. L. Foo, R. Matsuda, Y. Hijikata, R. Krishna, H. Sato, S. Horike, A. Hori, J. Duan, Y. Sato, Y. Kubota, M. Takata, S. Kitagawa, *J. Am. Chem. Soc.*, 2016, **138**, 3022-3030.
- [10] R. Eguchi, S. Uchida, N. Mizuno, *Angew. Chem. Int. Ed.*, 2012, **51**, 1635-1639.
- [11] W. Yang, A. J. Davies, X. Lin, M. Suyetin, R. Matsuda, A. J. Blake, C. Wilson, W. Lewis, J. E. Parker, C. C. Tang, M. W. George, P. Hubberstey, S. Kitagawa, H. Sakamoto, E. Bichoutskaia, N. R. Champness, S. Yang, M. Schroder, *Chem. Sci.*, 2012, **3**, 2993-2999.